Nanominerals, Mineral Nanoparticles, and Earth Systems

Michael F. Hochella Jr.,[1]* Steven K. Lower,[2] Patricia A. Maurice,[3] R. Lee Penn,[4] Nita Sahai,[5] Donald L. Sparks,[6] Benjamin S. Twining[7]

Minerals are more complex than previously thought because of the discovery that their chemical properties vary as a function of particle size when smaller, in at least one dimension, than a few nanometers, to perhaps as much as several tens of nanometers. These variations are most likely due, at least in part, to differences in surface and near-surface atomic structure, as well as crystal shape and surface topography as a function of size in this smallest of size regimes. It has now been established that these variations may make a difference in important geochemical and biogeochemical reactions and kinetics. This recognition is broadening and enriching our view of how minerals influence the hydrosphere, pedosphere, biosphere, and atmosphere.

Most physical, chemical, and biological processes on Earth are either influenced to some degree or fully driven by the properties of minerals. But with only about 4500 mineral species presently described, not many relative to millions of prokaryotic and eukaryotic species combined, their diversity and range of influence may seem, by comparison, relatively modest. Minerals exert their influence by constituting the bulk of this rocky planet and having a wide range of composition and structure that is expressed in a marked diversity of physical and chemical properties. Now we are gaining a much better appreciation for another aspect of mineral diversity—that which is expressed in the nanoscale size range (1–3). Here, atomic and electronic structure of nanoparticles may vary with size even without a phase transformation, and surface-to-volume ratios change dramatically. Such particles are minerals that are as small as roughly 1 nm and as large as several tens of nanometers in at least one dimension. Limiting size in one, two, or three dimensions results in a nanofilm (or nanosheet), a nanorod, or a nanoparticle, respectively. Minerals can be found in all of these shapes, although this review will concentrate on nanoparticles. Nanominerals are defined here as minerals that only exist in this size range; that is, one will not find their

equivalent at sizes larger than this. Well-known examples include certain clays as well as iron and manganese (oxyhydr)oxides (with ferrihydrite, an iron oxyhydroxide, as a type example). Mineral nanoparticles are minerals that can also exist in larger sizes, and these probably include most of all known minerals.

The importance of certain types of nanominerals and mineral nanoparticles, namely clays

and the smallest mineral colloids, has been known for a long time. What has been generally recognized more recently is that nanominerals and mineral nanoparticles commonly behave differently as a function of their size within the nanoscale size range. Mineral nanoparticles also behave differently than larger micro- and macroscopic crystals of the same mineral. This observation violates aspects of the long-standing, formal definition of a mineral. Although definitions vary somewhat, depending on the source, the general consensus is that minerals are naturally occurring, crystalline substances having a characteristic and defined chemical composition (or compositional range in the case of solid solutions). For any particular composition, each mineral expresses a set of specific physical and chemical properties. Nanominerals and mineral nanoparticles satisfy these criteria, except that even with a fixed composition, they express a range of physical and chemical properties depending on their size and shape.

Origin, Occurrence, and Distribution

Under the influence of either abiotic or biotic processes, all minerals go through a nanophase stage during formation. In most cases, this stage is transitory. But in cases where nucleation rates are high and growth rates are slow, as well as
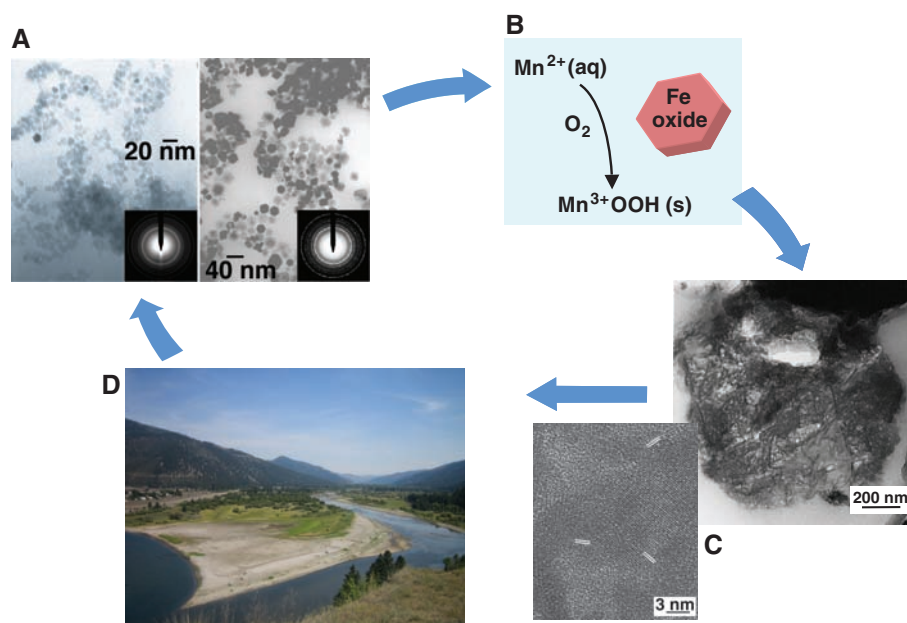
[1]Center for NanoBioEarth, Department of Geosciences, Virginia Polytechnic Institute and State University (Virginia Tech), Blacksburg, VA 24061–0420, USA. [2]School of Earth Sciences and School of Environment and Natural Resources, Ohio State University, Columbus, OH 43210, USA. [3]Department of Civil Engineering and Geological Sciences, University of Notre Dame, Notre Dame, IN 46556, USA. [4]Department of Chemistry, University of Minnesota, Minneapolis, MN 55455, USA. [5]Department of Geology and Geophysics, University of Wisconsin-Madison, Madison, WI 53706–1692, USA. [6]Center for Critical Zone Research, Department of Plant and Soil Sciences, University of Delaware, Newark, DE 19717–1303, USA. [7]Department of Chemistry and Biochemistry, University of South Carolina, Columbia, SC 29208, USA.

*To whom correspondence should be addressed. E-mail: hochella@vt.edu

Fig. 1. An example of the cycle of nanomineralogy and nanogeoscience research. (**A**) Mineral nanoparticles (hematite, in this case) of different sizes and/or shapes are synthesized (23) so that they can be systematically studied. (**B**) Wet chemical experiments that simulate some aspect of interest in a natural setting are run; in this case, hematite nanoparticles are used to catalyze the oxidation of aqueous Mn^{2+}, resulting in the formation of a manganese oxyhydroxide (23). (**C**) Examples may be found in nature (42) that closely compare to systems studied in the lab (23); a Mn hydrous oxide nanomineral (a vernadite-like phase making up the darker areas and "strings" in the image to the right; nanocrystals of this mineral are shown at high resolution in the image to the left), which is intimately associated with ferrihydrite (the medium gray areas in the image to the right), contains relatively high concentrations of several toxic heavy metals and is important in toxic metal transport in the Clark Fork River Superfund Complex in Montana (**D**). With field observations, laboratory experiments are refined or created anew [back to (A)].

where aggregated growth of mineral nanoparticles (4) is not a dominant process, nanominerals and mineral nanoparticles will form and can persist. Mineral nanophases forming under biotic processes, or nanobiomineralization, may involve bacterially driven redox reactions of aqueous species associated with some cell function, such as sequestering a toxic metal or storing a micronutrient, which often result in nanosize minerals (5, 6). Mineral weathering also commonly generates nanosized primary or secondary phases.

Nanominerals and mineral nanoparticles are common and widely distributed throughout the atmosphere, oceans, groundwater and surface waters, soils, in and/or on most living organisms, and even within proteins such as ferritin. Their occurrence is more limited in crustal or mantle rocks, but they do exist in these rocks, and they can even influence deep Earth processes. Although the overall mass distribution of nanominerals and mineral nanoparticles in the Earth system is not known at this time, the oceans may be the principal reservoir for them. Riverine, glacial, and aeolian supplies of nanoparticles to the world's oceans are large, with global biogeochemical consequences (7, 8).

In the atmosphere, the mass of mineral dust derived annually from windblown arid and semiarid lands, and secondarily from agricultural lands, far exceeds the average mass of mineral dust derived from volcanic emissions, as well as biological debris (9). The only large atmospheric inputs of natural particles that rival all of these sources are the halite and hydrous sulfate aerosols from sea spray (10). The total volume of atmospheric mineral particles is dominated by particles that are larger than 100 nm, but numerically, most are nanoparticles less than 50 nm in size (11). The cumulative surface area of these nanoparticles is considerably less than that of the larger particles, but it is still notable (11). Mineral dust, including mineral nanoparticles, is distributed globally from its source regions by way of atmospheric circulation patterns. Climate change is projected to play the key role in variations of mineral dust origins and distribution patterns of the future (12, 13).

In addition to mineral growth or weathering, nanoparticles can be generated by mechanical grinding associated with earthquake-generating faults in Earth's crust. The presence of fault-related fine-grained rock fragments, containing mineral nanoparticles down to 10 to 20 nm in size, is likely to be important in fault mechanics (14, 15). Nanomineralogy is also important in places where the presence of nanominerals and mineral nanoparticles would not necessarily be anticipated. For example, nanoparticles of the high-pressure silicates ringwoodite and wadlye-

ite play a central role in deep-focus earthquakes at ~ 300 to 700 km depths in Earth's mantle (16).

Beyond Earth, the presence of nanophase ferric oxides in martian soils and airborne dust has been suspected for several years based on data from spectral imagers onboard the Mars Viking and Pathfinder landers, as well as ground-based observations (17, 18). In chondritic meteorites and interplanetary dust particles, minute concentrations of diamond nanoparticles exist. These nanodiamonds are thought to represent presolar dust, likely forming in supernovae, but it is also suggested that they could form directly in the solar nebula (19) and in conjunction with other star types (20). Nanodiamonds average 3 nm in diameter, and grains as small as 1 nm (<150 carbon atoms) have been observed (19).

Changes That Occur with Mineral Size

Current evidence suggests that—as with non-mineral metals, semiconductors, and insulating nanoparticles—nanominerals and mineral nanoparticles may show variations in their atomic structure relative to larger particles and as a function of size in the nanoscale regime (2, 5, 6). Many factors may be involved in these variations, including structurally disordered, strained, and/or reconstructed surfaces, as well as potential variations in surface topography and crystallographic surfaces that are exposed. Electronic structure variations are also expected, as observed for many other nanomaterials.

In small mineral nanoparticles, even the interior structure may be appreciably affected. Using a combination of extended x-ray absorption fine structure, wide-angle x-ray scattering, and pair distribution analyses, Gilbert and others (21) found that the atomic structure of 3.4-nm-diameter sphalerite (ZnS) nanoparticles deviated from that of bulk sphalerite, even though the surface was strongly passivated by a complexing ligand. A loss of structural coherence occurred at distances greater than 2 nm, suggesting that disrupted surface environments drive inhomogeneous internal strain. This results in structural stiffening that far exceeds what is expected by the mild overall bond-length contraction that is observed.

An example of structural variation as a function of particle size in the nanoregime can be garnered from a study of the nanomineral ferrihydrite (22), a common iron oxyhydroxide found in soils, oceans, surface waters, and groundwater. Individual crystallites of ferrihydrite are typically rounded and less than 10 nm in diameter. Pair distribution function analysis, derived from total x-ray scattering experiments and also calculated from refined atomic structure models, was used to gain insight into the structure of this important yet enigmatic phase. The results suggest that ferrihydrites with scattering domain sizes of 6, 3, and 2 nm have the same basic chemistry [$Fe_{10}O_{14}(OH)_2$], crystal structure with space group $P6_3mc$, cell dimensions a = ~5.95 Å
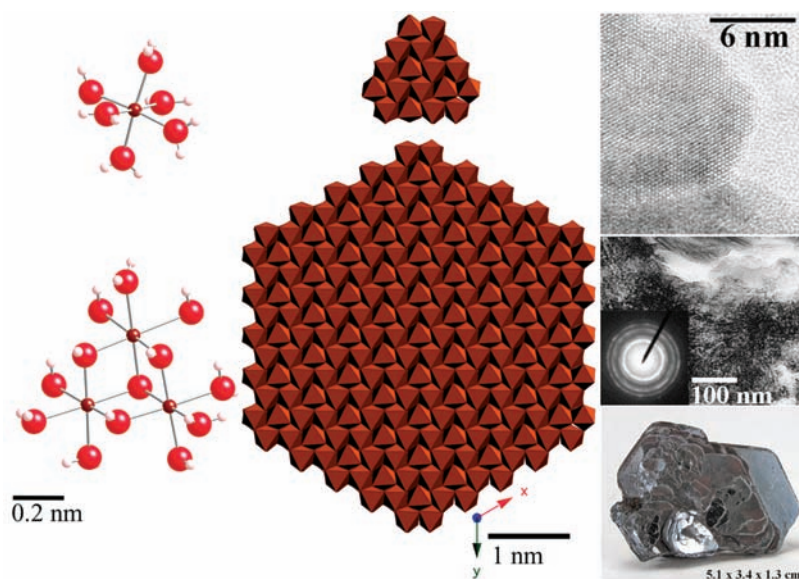

Fig. 2. Examples of how ferric iron occurs in the environment, ranging from the molecular to macroscopic scales. (**Left**) Molecular ferric oxide states, including an octahedrally coordinated monomer [hexaquairon III (53), top] and oligomer [trimer cluster (54), bottom] with Fe^{3+} (smaller dark red spheres), oxygen (larger light red spheres), and hydrogen (light pink spheres). These molecules are hydrogen-terminated but should only be considered approximations of actual aqueous/environmental states. (**Middle**) Polyhedral representations of 1- and 5-nm hematite (Fe_2O_3) nanoparticles. Each polyhedron represents an Fe^{3+} in octahedral coordination with oxygen. The thickness of the 5-nm particle should be typically several (roughly five to seven) octahedral layers (23) and that of the 1-nm particle should be just a few octahedral layers. (**Right**) (Top) HRTEM image of hematite nanoparticles from Namibia (Africa) (sample courtesy of the Smithsonian Institution research collection); (Middle) TEM image of an unoriented aggregate of 3- to 5-nm hematite crystals (stippled portion of the image) from an acid mine drainage site in Montana (USA) (55); (Bottom) photograph of macroscopic specular hematite (courtesy of R. Lavinsky).

and c = ~9.06 Å, and an 80/20 ratio of octahedrally to tetrahedrally coordinated iron. However, as this nanomineral becomes smaller, the a cell edge increases slightly (by 0.03 Å), the c cell edge decreases much more (by 0.16 Å), two of the three crystallographically distinct Fe sites show a decrease in occupancy, and the third Fe site (octahedral) remains fully occupied but shows increasing degrees of distortion. Like sphalerite nanoparticles (21), the atomic structure of ferrihydrite crystallites is probably influenced by surface relaxation driving internal disorder and strain (22). It is also interesting to consider that the 2-nm particles of ferrihydrite only contain ~ 20 unit cells, so a much higher percentage of Fe sites is at or near the surface versus that in the 6-nm particles with ~30 times the volume.

The Size Range of Nanominerals and Mineral Nanoparticles

The upper size range of nanominerals is likely to be quite variable, depending on the mineral. The upper size limit of mineral nanoparticles can be defined as the size above which the properties of the particles are indistinguishable from those of the bulk material, or (equivalently) the size where, as the mineral particles become smaller and smaller, properties begin to show variations relative to those of larger particles of the same mineral. This size should depend on the nature of the material (e.g., whether it is a metal, semiconductor, or insulator), the particle shape, and the property measured (e.g., whether it is chemical, electrical, optical, mechanical, or thermodynamic). In most cases, it is not known below what size these properties will begin to vary for which minerals, because, to date, few measurements of this type have been made. In a few cases where this information exists for affinities and rates of geochemically relevant reactions for certain iron oxide minerals, it has been suggested that surface area–normalized variations are observed when size drops below a few tens of nanometers (23–26).

The lower size limit of nanominerals and mineral nanoparticles is also challenging to delineate. Minerals, by definition, are crystalline, which requires a repeating arrangement of atoms. Therefore, the smallest atomic clusters cannot qualify as nanominerals or mineral nanoparticles, but an atomic arrangement that is greater than a few unit cells in one or more dimensions would qualify. Using zinc, sulfur, and the mineral sphalerite as an example, one can start with an individual zinc ion dissolved in water: the hexaquo Zn complex $[Zn^{2+}(H_2O)_6]$. In the presence of dissolved reduced sulfur, ZnS cluster complexes can form, for example, with the stoichiometry of $Zn_3S_3(H_2O)_6$ (27). Molecular modeling of this cluster shows that it has a diameter of about 0.7 nm (27). A single unit cell of sphalerite, containing Zn_4S_4, has a cubic unit-cell dimension of 0.54 nm with an atomic density greater than that of the cluster. The smallest nanoparticles of sphalerite that have been observed to date are

about 1.5 nm in size, although there is no a priori reason not to expect smaller ones (5). From this analysis, one should expect the smallest sphalerite nanoparticles to be in the neighborhood of 1 nm in size, with larger ZnS cluster complexes also in this size range.

Reactivity and Stability

With variations in surface and near-surface atomic structure as a function of size, one can anticipate a concomitant change in the chemical interactions of nanominerals and mineral nanoparticles with their environment that does not scale with the total available surface area. Examples of this include the following (all rates are surface area–normalized): 7-nm hematite (α-Fe$_2$O$_3$) nanocrystals catalyze the oxidation of aqueous Mn^{2+} one to two orders of magnitude faster than 37-nm hematite crystals (23), resulting in the rapid formation of Mn oxide minerals that are important heavy metal sorbents in water and soils; hydroquinone-driven reductive dissolution reactions of 5 × 64 nm goethite (α-FeOOH) are twice as fast compared with those of 22 × 367 nm goethite (24); 7-nm hematite shows a significantly increased sorption affinity for aqueous Cu^{2+} versus that of 25- and 88-nm hematite (25); and the reduction rate of hematite by *Shewanella oneidensis* MR-1 with lactate as the sole electron donor is an order of magnitude faster for 99-nm versus 11-nm nanoparticles (26).

Thermodynamic considerations in the nanorange are just as fascinating and critical to consider if we are to have a means for predicting the stability of nanophases under various Earth conditions, as well as to understand polymorphic phase transformations driven by size. Toward these goals, surface enthalpies of nanominerals and mineral nanoparticles, as well as enthalpies of phase transitions, have been measured for polymorphs of Al, Fe, Mn, Ti, and Zr oxides via high-temperature oxide-melt solution calorimetry and water adsorption calorimetry (28–30). At the nanoscale, three factors compete to stabilize a given polymorph: enthalpy of polymorphic transition, surface enthalpy, and enthalpy of hydration. In general, the polymorphs metastable for coarse particles have lower surface energies, leading to crossovers in phase stability as the particle size decreases. This provides a thermodynamic explanation of why nanoparticulate oxides often crystallize as one polymorph, whereas another polymorph is exhibited in coarser-grained material. It is important for future studies to make the thermodynamic predictions more relevant to Earth systems and to obtain systematic size-resolved thermodynamic data for systems of geochemical importance, including clays and carbonates.

Mineral solubility is a crucial property in predicting the fate of minerals and dissolved species in the environment. A modified version of the Kelvin equation predicts solubility dependence on size, stating that as particles get smaller through the nanorange of sizes, their

solubilities increase exponentially (6). This implies that mineral nanoparticles in a dissolution setting would have short life-spans. However, it is not known how generally applicable this relationship is for minerals. Certain minerals are known to become less soluble as they get smaller (31). In addition, mineral nanoparticles of lepidocrocite (an iron oxyhydroxide) and FePO$_4$·nH$_2$O have been formed at lower Fe/P ratios in solution than predicted by their bulk solubilities (32). This same study shows that in aqueous binary and ternary systems of Fe + PO$_4$ ± As, mixed nanophase coprecipitates form with the compositions Fe[(OH)$_3$, PO$_4$]·nH$_2$O and Fe[(OH)$_3$, AsO$_4$, PO$_4$]·nH$_2$O. These nanophases do not have bulk counterparts or known solubilities. They are distinct from ferrihydrite or lepidocrocite with sorbed PO$_4$ and AsO$_4$, and are very similar to mixed, metastable nanophases found in certain natural sedimentary environments (32).

Influence on Earth Chemistry

We start with an example that involves phytoplankton production levels in the open oceans, a process that provides a connection between nanoparticles, oceans, and global atmospheric and hydrospheric chemistry. Ocean phytoplankton play a critical role in influencing the amount of CO$_2$ in the atmosphere, and phytoplankton growth in large swaths of the global ocean has been shown to be limited by iron availability. Dissolved inorganic and organic complexes are typically thought to comprise the bioavailable pool of iron in the ocean. However, recent studies indicate that a significant fraction of the "dissolved" (<0.4 μm) iron in the ocean is actually composed of iron colloids and nanoparticles (33, 34). Furthermore, this fraction contributes much of the observed variability in dissolved ocean iron concentrations (35). Oceanographic studies have typically used ultrafiltration membranes to define colloidal iron as the fraction greater than 20 to 25 nm, but researchers using electron microscopy have noted the presence of 2- to 20-nm particles at even higher concentrations (>10^9 ml^{-1}) (36, 37). These particles appear to consist of organic compounds surrounding 2- to 5-nm mineral nanoparticles (38). Recent studies with high-resolution transmission electron microscopy (HRTEM) and electron energy-loss spectroscopy, however, have positively identified iron (oxyhydr)oxide nanoparticles 5 to 20 nm in diameter in glacial and riverine sediments (7, 8). Iron associated with windblown mineral dust, including nanoparticulate dust, is also an important micronutrient input for phytoplankton (13). The input of iron within nanoparticles to the oceans has been estimated to far exceed riverine input of dissolved iron (39). Further, recent evidence suggests that iron within particulates contained in glacial sediments is bioavailable to marine phytoplankton and that this may be an increasingly important source in this century as icebergs are ejected from Antarctic shelves (40). Laboratory experiments

have shown that iron oxide nanoparticles can support the growth of osmotrophic phytoplankton after photoreduction or thermal dissolution (*41*), whereas mixotrophic phytoplankton may access mineral nanoparticles through direct ingestion (*42*).

Nanophase minerals also influence the movement of harmful heavy metals in Earth's near-surface environment via complex interactions involving rock, soil, water, air, and living organisms, in many cases overprinted by anthropogenic processes. For instance, lead, arsenic, copper, and zinc were mobilized over hundreds of kilometers within the Clark Fork River drainage basin, part of which makes up the Clark Fork River Superfund Complex in western Montana, the largest Superfund site in the United States. These metals are incorporated into and transported by a newly discovered nanocrystalline vernadite-like mineral (a manganese oxyhydroxide) along major portions of the river (*43*). This nanomineral likely forms as a result of the catalytic oxidation of aqueous manganese on ferrihydrite surfaces (*23*) (Fig. 1).

The movement of radionuclides (and other toxic metals) in the subsurface often defies laboratory- and thermodynamically based predictions that they should be essentially immobile (*44*). It has been shown that radionuclides can be carried over many kilometers in relatively short periods of time by colloids moving with groundwater. At a nuclear waste reprocessing plant in Mayak, Russia (one of the most contaminated nuclear sites in the world), plutonium has traveled several kilometers in the local groundwater system; 70 to 90% of the plutonium transport was attributed to nanoparticles less than 15 nm in size in the groundwater (*45*). The nanocarriers in this instance were primarily ferric iron oxides (not clays, calcite, rutile, or other nanomineral and mineral nanoparticle colloids that were also present).

The size dependence of the properties of atmospheric nanoparticles is just beginning to be explored. For example, atmospheric mineral nanoparticles [typically halite (NaCl) and hydrous sulfate evaporates from sea spray] are hygroscopic and act as water droplet nucleation and growth centers. This is a critical step in cloud formation. The size and density of the droplets dictate the solar radiation scattering ability and longevity of clouds, both important factors in influencing average global temperatures. The hygroscopic growth factor for NaCl nanoparticles decreases for sizes below 40 nm as a result of a size-dependent shape factor and the Kelvin effect that takes into account the change in surface tension as a function of surface curvature (*46*). Therefore, only relatively large mineral nanoparticles (>40 nm) are expected to contribute to cloud condensation nuclei.

Although minerals can carry human irritants and toxic materials in the atmosphere, many carriers are from anthropogenic sources, most notably particulates emitted from the combustion of fossil fuels (*47*) and many other emissions

from the vast numbers of industries that are associated with metals (*48*). Many trace metals in airborne particles, including highly toxic metals such as cadmium, lead, and arsenic, occur in the very fine (<1-µm) to ultrafine (<100-nm) size fraction (*48*, *49*), and their distinctive properties will influence the bioavailability of the metals in these particles.

Elemental distribution and bioavailability, reaction pathways and catalysis, and mineral growth/solubility/weathering are all influenced by phenomena relevant to, with no equivalent phenomena at scales larger or smaller than, the nanoscale. A dissolved ion in aqueous solution behaves differently than that same ion in a 1-nm mineral, and both behave differently than that same ion in a 5-nm or larger mineral. Considering everything that passes through 200- or 2-nm filters as dissolved is not appropriate. Aqueous and gas-based reactions that occur on (or in conjunction with) a molecular cluster versus a small mineral nanoparticle versus a 50-nm or larger mineral particle, all with equivalent compositions (depicted in Fig. 2), are predicted to most often show significantly different pathways and kinetics.

Challenges for the Future

Measuring and understanding nanomineral and mineral nanoparticle origin (biotic or abiotic, natural or anthropogenic), geographic distribution, relevant nanochemistry, and overall influence and impact within the complex chemical and physical framework of Earth systems are all critical challenges for the future. For example, it is still not known whether metal oxide and other potentially catalytically active airborne nanoparticles can significantly modify atmospheric chemistry, even locally, as a result of nanomineral-gas heterogeneous chemical reactions (*11*). It is possible that important reactions may be driven under these specific circumstances and no other atmospheric scenario, especially where aerosols with very high nanomineral or mineral nanoparticle surface areas exist, or where reaction kinetics would be highly favorable on their surfaces. Very little information presently exists in this field. However, if discovered, such findings may be of fundamental interest and importance, much as was the discovery of the production of ozone-destroying chlorine compounds on the surface of polar stratospheric cloud aerosols (*50*).

The same general types of challenges remain in terrestrial and ocean systems. In addition, because nanoparticle aggregation is common in aqueous environments, one must also consider the formation and dispersion of aggregated states, and the transport of reactants to and products from reactive sites within aggregates. Further, when nanoparticles aggregate, it will be important to determine which properties are controlled by individual particles and which by the aggregate as a whole, and how the properties may change as aggregates form and dissociate.

All the complexities of nanomineral and mineral nanoparticle composition, structure, stability, and reactivity also apply to the human body, where normal and pathological mineralization (from the nanosize to the micron-size) affects the calcification of bones, teeth, arteries, and veins, as well as the formation of stones in the kidneys and joints (*51*). An equally important field is called nanotoxicology, defined as the safety evaluation of engineered nanostructures through a knowledge of the mechanisms and biokinetics of nanomaterials causing adverse effects in humans (*52*). The enormous impact of asbestos–human lung interactions gives some idea of the scope and importance of this one subfield. Nanominerals and mineral nanoparticles in the environment have been present throughout the evolutionary development of hominids, and our exposure to these through inhalation, ingestion, and dermal pathways are important foci of nanotoxicology.

The biogeochemical and ecological impacts of natural and synthetic nanomaterials are some of the fastest growing areas of research today, with not only vital scientific but also large environmental, economic, and political consequences (*3*).

References and Notes

1. J. F. Banfield, A. Navrotsky, Eds. *Nanoparticles and the Environment* (Mineralogical Society of America, Washington, DC, 2001).
2. G. A. Waychunas, C. S. Kim, J. F. Banfield, *J. Nanopart. Res.* **7**, 409 (2005).
3. N. S. Wigginton, K. L. Haus, M. F. Hochella Jr., *J. Environ. Monit.* **9**, 1306 (2007).
4. R. L. Penn, J. F. Banfield, *Science* **281**, 969 (1998).
5. J. F. Banfield, H. Zhang, in (*1*), pp. 1–58.
6. B. Gilbert, J. F. Banfield, in *Molecular Geomicrobiology*, J. F. Banfield, J. Cervini-Silva, K. H. Nealson, Eds. (Mineralogical Society of America, Chantilly, VA, 2005), pp. 109–155.
7. S. W. Poulton, R. Raiswell, *Chem. Geol.* **218**, 203 (2005).
8. R. Raiswell *et al.*, *Geochim. Cosmochim. Acta* **70**, 2765 (2006).
9. J. H. Seinfeld, S. N. Pandis, *Atmospheric Chemistry and Physics* (Wiley, New York, 1998).
10. C. D. O'Dowd, M. H. Smith, I. E. Consterdine, J. A. Lowe, *Atmos. Environ.* **31**, 73 (1997).
11. C. Anastasio, S. T. Martin, in (*1*), pp. 293–349.
12. I. Tegen, M. Werner, S. P. Harrison, K. E. Kohfeld, *Geophys. Res. Lett.* **31**, L05105 (2004).
13. J. M. Prospero, P. J. Lamb, *Science* **302**, 1024 (2003).
14. B. Wilson, T. Dewers, Z. Reches, J. Brune, *Nature* **434**, 749 (2005).
15. O. Dor, Y. Ben-Zion, T. K. Rockwell, J. Brune, *Earth Planet. Sci. Lett.* **245**, 642 (2006).
16. H. W. Green II, P. C. Burnley, *Nature* **341**, 733 (1989).
17. J. F. Bell III *et al.*, *J. Geophys. Res.* **105**, 1721 (2000).
18. R. V. Morris *et al.*, *J. Geophys. Res.* **105**, 1757 (2000).
19. Z. R. Dai *et al.*, *Nature* **418**, 157 (2002).
20. A. B. Verchovsky *et al.*, *Astrophys. J.* **651**, 481 (2006).
21. B. Gilbert, F. Huang, H. Zhang, G. A. Waychunas, J. F. Banfield, *Science* **305**, 651 (2004).
22. F. M. Michel *et al.*, *Science* **316**, 1726 (2007).
23. A. S. Madden, M. F. Hochella Jr., *Geochim. Cosmochim. Acta* **69**, 389 (2005).
24. A. J. Anschutz, R. L. Penn, *Geochem. Trans.* **6**, 60 (2005).
25. A. S. Madden, M. F. Hochella Jr., T. P. Luxton, *Geochim. Cosmochim. Acta* **70**, 4095 (2006).
26. S. Bose *et al.*, in *Abstracts of Papers*, 232nd National Meeting of the American Chemical Society, San Francisco,

10 to 14 September, 2006 (American Chemical Society, Washington, DC, 2006).

27. G. W. Luther, D. T. Rickard, *J. Nanopart. Res.* **7**, 389 (2005).
28. A. Navrotsky, in (*1*), pp. 73–103.
29. A. Navrotsky, *J. Chem. Thermodyn.* **39**, 2 (2007).
30. A. Navrotsky, L. Mazeina, J. Majzlan, *Science* **319**, 1635 (2008).
31. R. K. Tang, L. J. Wang, G. H. Nancollas, *J. Mater. Chem.* **14**, 2341 (2004).
32. N. Sahai, Y. Lee, H. Xu, M. Ciardelli, J.-F. Gaillard, *Geochim. Cosmochim. Acta* **71**, 3193 (2007).
33. J. Wu, E. Boyle, W. Sunda, L.-S. Wen, *Science* **293**, 847 (2001).
34. J. Nishioka, S. Takeda, C. S. Wong, W. K. Johnson, *Mar. Chem.* **74**, 157 (2001).
35. B. A. Bergquist, J. Wu, E. A. Boyle, *Geochim. Cosmochim. Acta* **71**, 2960 (2007).
36. M. L. Wells, E. D. Goldberg, *Nature* **353**, 342 (1991).
37. M. L. Wells, E. D. Goldberg, *Limnol. Oceanogr.* **39**, 286 (1994).
38. M. L. Wells, E. D. Goldberg, *Mar. Chem.* **40**, 5 (1992).
39. S. W. Poulton, R. Raiswell, *Am. J. Sci.* **302**, 774 (2002).
40. K. L. Smith *et al.*, *Science* **317**, 478 (2007).
41. H. W. Rich, F. M. M. Morel, *Limnol. Oceanogr.* **35**, 652 (1990).
42. L. M. Nodwell, N. M. Price, *Limnol. Oceanogr.* **46**, 765 (2001).
43. M. F. Hochella Jr., T. Kasama, A. Putnis, C. Putnis, J. N. Moore, *Am. Mineral.* **90**, 718 (2005).
44. W. R. Penrose *et al.*, *Environ. Sci. Technol.* **24**, 228 (1990).
45. A. P. Novikov *et al.*, *Science* **314**, 638 (2006).
46. G. Biskos, L. M. Russell, P. R. Buseck, S. T. Martin, *Geophys. Res. Lett.* **33**, L07801 (2006).
47. M. Zheng *et al.*, *Atmos. Environ.* **39**, 3967 (2005).
48. S. Utsunomiya, K. A. Jensen, G. J. Keeler, R. C. Ewing, *Environ. Sci. Technol.* **38**, 2289 (2004).
49. L. E. Murr, J. J. Bang, *Atmos. Environ.* **37**, 4795 (2003).
50. M. J. Molina, T. Tso, L. T. Molina, F. C. Wang, *Science* **238**, 1253 (1987).
51. N. Sahai, M. A. A. Schoonen, Eds. *Medical Mineralogy and Geochemistry* (Mineralogical Society of America, Chantilly, VA, 2006).
52. G. Oberdörster, E. Oberdörster, J. Oberdörster, *Environ. Health Perspect.* **113**, 823 (2005).
53. C. Junk *et al.*, *J. Chem. Soc. Dalton Trans.* **2002**, 1024 (2002).
54. K. M. Rosso, E. S. Ilton, *J. Chem. Phys.* **119**, 9207 (2003).
55. M. F. Hochella Jr., J. N. Moore, U. Golla, A. Putnis, *Geochim. Cosmochim. Acta* **63**, 3395 (1999).
56. We thank NSF, Directorate for Geosciences, for sponsoring the Nanogeosciences Working Group from which this paper originated. Support was also provided by NSF grants EAR02-21966 (Environmental Molecular Science Institute), DGE-0504196 (Integrative Graduate Education and Research Traineeship Program) CAREER-0346385, EAR-0346889, EAR-0525297, EAR-0544246, and OCE-0527062; U.S. Department of Energy grants DE-FG02-02ER15323 and DE-FG02-06ER15786; U.S. Department of Agriculture grant USDA 2005-35107-16105; and the Institute for Critical Technology and Applied Science at Virginia Tech. We acknowledge two anonymous reviewers for many important suggestions that improved this manuscript, as well as S. Bose, H. Green II, B. Lower, A. Madden, R. Mahajan, A. Navrotsky, and N. Woodward for many useful discussions.

Size-Driven Structural and Thermodynamic Complexity in Iron Oxides

Alexandra Navrotsky,[1]* Lena Mazeina,[2] Juraj Majzlan[3]

Iron oxides occur ubiquitously in environmental, geological, planetary, and technological settings. They exist in a rich variety of structures and hydration states. They are commonly fine-grained (nanophase) and poorly crystalline. This review summarizes recently measured thermodynamic data on their formation and surface energies. These data are essential for calculating the thermodynamic stability fields of the various iron oxide and oxyhydroxide phases and understanding their occurrence in natural and anthropogenic environments. The competition between surface enthalpy and the energetics of phase transformation leads to the general conclusion that polymorphs metastable as micrometer-sized or larger crystals can often be thermodynamically stabilized at the nanoscale. Such size-driven crossovers in stability help to explain patterns of occurrence of different iron oxides in nature.

It is hard to find a process or environment in which iron oxides do not participate. From the surface of Mars to the depths of Earth, from old rusting factories to high-tech magnetic recording devices, from pigeon brains and magnetotactic bacteria to drug delivery systems, anhydrous and hydrated iron oxides are ubiquitous. They are constituents of rocks and soils, products of corrosion and bacterial processes, and sources of iron as a nutrient. They have many commercial applications: pigments, catalysts, medical devices, sensors, and recording media. Nanotechnology increasingly makes use of iron oxide nanoparticles and thin films.

Iron oxides exist in a bewildering variety of polymorphs (*1*). Anhydrous ferric oxides include hematite (α-Fe$_2$O$_3$), maghemite (γ-Fe$_2$O$_3$), and the less common ε- and β-Fe$_2$O$_3$. Fe$_3$O$_4$ (magnetite) and Fe$_{1-x}$O (wüstite) contain both ferric and ferrous iron. Maghemite and magnetite, both spinels, can form a continuous solid solution. The oxyhydroxides, nominally FeOOH, include goethite, lepidocrocite, akaganeite, and several other polymorphs. They often contain excess water. More hydrated forms such as ferrihydrite, nominally Fe(OH)$_3$, have even more variable water content. Hydrated phases containing both ferrous and ferric iron include the green rusts, layered hydroxides with different anions in the interlayer. A further complication is that many iron oxides, both in nature and in the laboratory, are exceedingly fine-grained (nanophase) and therefore hard to characterize.

This complexity has meant that until recently, knowledge of the structural details, thermodynamics, and reactivity of iron oxides has been lacking. One could not understand or predict which phases form under what conditions, which polymorphs are stable and which metastable, and

[1]Peter A. Rock Thermochemistry Laboratory and Nanomaterials in the Environment, Agriculture, and Technology Organized Research Unit, University of California, Davis, CA 95616, USA. [2]Naval Research Laboratory, Washington, DC 20375, USA. [3]Institute of Mineralogy, Petrology and Geochemistry, Albert-Ludwigs-Universität Freiburg, D-79104 Freiburg, Germany.

*To whom correspondence should be addressed. E-mail: anavrotsky@ucdavis.edu

Table 1. Thermodynamic data for iron oxides. Enthalpies of formation (ΔH_f°) and Gibbs free energies of formation (ΔG_f°) are for conditions of 298 K and 1 bar. Surface enthalpies are given for anhydrous (ΔH_s) and hydrated (ΔH_s^h) surfaces. Most of the data are taken from the references cited. Values of Gibbs free energy without citations were calculated from corresponding values of standard enthalpies and entropies.

Oxide	ΔH_f° (kJ mol^{-1})	S° (J mol^{-1} K^{-1})	ΔS_f° (J mol^{-1} K^{-1})	ΔG_f° (kJ mol^{-1})	ΔH_s^h (J m^{-2})	ΔH_s (J m^{-2})
Hematite, α-Fe$_2$O$_3$	−826.2 ± 1.3 (*31*)	87.4 ± 0.2 (*31*)	−274.5 ± 0.3 (*31*)	−744.4 ± 1.3 (*31*)	0.75 ± 0.16 (*13*)	1.9 ± 0.3 (*18*)
Maghemite, γ-Fe$_2$O$_3$	−811.6 ± 2.2 (*4*)	93.0 ± 0.2 (*17*)	−268.9 ± 0.3 (*17*)	−731.4 ± 2.0	0.57 ± 0.10 (*4*)	0.71 ± 0.13 (*4*)
ε-Fe$_2$O$_3$	−798 ± 7 (*15*)			−717.8 ± 6.6 (*15*)		
Goethite, α-FeOOH	−561.5 ± 1.5 (*12*)	59.7 ± 0.2 (*17*)	−237.9 ± 0.2 (*17*)	−490.6 ± 1.5	0.60 ± 0.10 (*12*)	0.91 ± 0.09 (*18*)
Lepidocrocite, γ-FeOOH	−552.0 ± 1.6 (*10*)	65.1 ± 0.2 (*17*)	−232.5 ± 0.2 (*17*)	−482.7 ± 3.1	0.40 ± 0.16 (*10*)	0.62 ± 0.14 (*10*)
Akaganeite, β-FeOOH	−554.7 ± 1.9 (*11*)	53.8 ± 3.3 (*32*)	−246.2 ± 3.3 (*32*)	−481.7 ± 1.9	0.34 ± 0.04 (*11*)	0.44 ± 0.04 (*11*)
Feroxyhyte, δ-FeOOH	−552.0 ± 1.0 (*13*)			−483.1 ± 1.3 (*13*)		
Ferrihydrite, Fe(OH)$_3$	−830.3 ± 2.0 (*15*)			−711.0 ± 2.0 (*15*)		